Green Tea Catechins Inhibit Bacterial DNA Gyrase by Interaction with Its ATP Binding Site

Helena Gradišar,[†,‡] Primož Pristovšek,[†,‡] Andreja Plaper,[§] and Roman Jerala*[,‡]

Laboratory of biotechnology, National Institute of Chemistry, Hajdrihova 19, 1000 Ljubljana, Slovenia, and KRKA Pharmaceutical Company, Šmarješka cesta 6, 8501 Novo mesto, Slovenia

Received July 12, 2006

Catechins are the main ingredients of green tea extracts and have been shown to possess versatile biological activities, including antimicrobial. We determined that the catechins inhibit bacterial DNA gyrase by binding to the ATP binding site of the gyrase B subunit. In the group of four tested catechins, epigallocatechin gallate (EGCG) had the highest activity, followed by epicatechin gallate (ECG) and epigallocatechin (EGC). Specific binding to the N-terminal 24 kDa fragment of gyrase B was determined by fluorescence spectroscopy and confirmed using heteronuclear two-dimensional NMR spectroscopy of the EGCG−^{15}N-labeled gyrase B fragment complex. Protein residues affected by binding to EGCG were identified through chemical shift perturbation. Molecular docking calculations suggest that the benzopyran ring of EGCG penetrates deeply into the active site while the galloyl moiety anchors it to the cleft through interactions with its hydroxyl groups, which explains the higher activity of EGCG and ECG.

Introduction

Widespread emergence of bacterial resistance to present drugs represents a serious problem in treatment of bacterial infections.[1] Modern approaches toward development of new potential inhibitors are based on knowledge of structure and function of proteins specific to bacteria. One of them is DNA gyrase, a characteristic and essential bacterial enzyme whose inactivation leads to bacterial death. For this reason, gyrases have been chosen as targets for antibacterial agents. Gyrases are members of the topoisomerase family of enzymes that are able to relax supercoiled DNA; however, only gyrases are also able to introduce supercoils into DNA in a reaction coupled to the hydrolysis of ATP. The active gyrase is a heterotetramer composed of two A and two B subunits. Subunit A (gyrase A) is involved in DNA breakage−resealing reactions, while subunit B (gyrase B) catalyzes ATP hydrolysis, providing the driving force for supercoiling of DNA. Both subunits have been investigated as targets for antibacterial drugs. A variety of gyrase inhibitors are known that predominantly act on gyrase A,[2,3] while coumarines and cyclothialidines act on gyrase B.[4] Known inhibitors of gyrase B are not in general medical use due to their toxicity in eukaryotic systems. Natural substances with antigyrase activities, such as those present in nutrients, are interesting as leads for the design of new antimicrobials due to their proven safety. Flavonoids as ubiquitous natural polyphenolic substances are common constituents of plants that are traditionally involved in human diet and herbal medicine. Green tea, a widely consumed beverage, has been shown to express numerous beneficial effects on human health. Dried tea leaves contain up to 30% of catechin-based polyphenols that display various physiological activities, such as radical scavenging action[5−8] and prevention of atherosclerosis.[5,9−11] Furthermore, several studies indicate that catechins inhibit carcinogenesis,[12,13] tumor growth,[14−17] cancer cell invasion and tumor angiogenesis[18,19] and also exhibit antimicrobial activity.[20−28] However, in most cases the mechanisms and even molecular targets of these activities are not clear. The antimicrobial activity of green tea catechins (reviewed in 29) has been previously assigned to interaction with either bacterial membrane or specific protein targets.[30−32] Recently, particular bacterial enzymes such as fatty acid synthase[33] or beta lactamase[27] have been identified as possible targets.

The major constituents of green tea (*Camellia sinensis*) extract are catechin-based flavonoids (Figure 1). Among them, (−)-epigallocatechin-3-gallate (EGCG[a]) is the most abundant (40−60%), followed by (−)-epicatechin-3-gallate (ECG, 10−20%), (−)-epigallocatechin (EGC, 10−20%), and (−)-epicatechin (EC, 4−6%); in sum, they contribute to more than 200 mg of catechins per cup of green tea. In our study, we examined the inhibitory effect of four related catechins on bacterial gyrase B. The catechins EGCG, EGC, ECG, and EC were evaluated for their ability to inhibit the ATPase activity, and their binding affinity for gyrase B was determined. NMR structural experiments were performed, providing information for *in silico* molecular docking experiments and contributing to the structural background of catechin interaction with their targets.

Results

Binding of Catechins to the 24 kDa Fragment of Gyrase B (G24). Catechins from green tea have been shown before to bind to and inhibit kinases[34,35] as well as to display antimicrobial activity. The ATP-binding site of gyrase B that resides within the N-terminal 24 kDa domain[4,36,37] shares structural similarity with several other ATP-binding proteins,[38,39] which prompted us to examine binding of catechins to DNA gyrase. We have shown previously that quercetin binds to the ATP-binding site of G24 with a K_d of 15 μM and that its fluorescence increases significantly in this complex.[37] The catechins used in this study are not fluorescent; consequently, we have chosen displacement of fluorescent quercetin for monitoring the competitive binding of the catechins to G24. The intensity of the quercetin fluorescence decreased when EGCG, EGC, ECG, or EC were added to the solution containing the G24−quercetin complex (Figure 2A). These changes prove that quercetin was displaced

* To whom correspondence should be addressed. Tel./Fax: +396 1 4760 335/300. E-mail: roman.jerala@ki.si.
† These authors contributed equally to this work.
‡ National Institute of Chemistry.
§ KRKA Pharmaceutical Company.

[a] Abbreviations: EC, (−)-epicatechin; EGC, (−)-epigallocatechin; ECG, (−)-epicatechin gallate; EGCG, (−)-epigallocatechin-3-gallate; G24, N-terminal 24 kDa fragment of gyrase B.

10.1021/jm060817o CCC: $37.00
Published on Web 12/21/2006

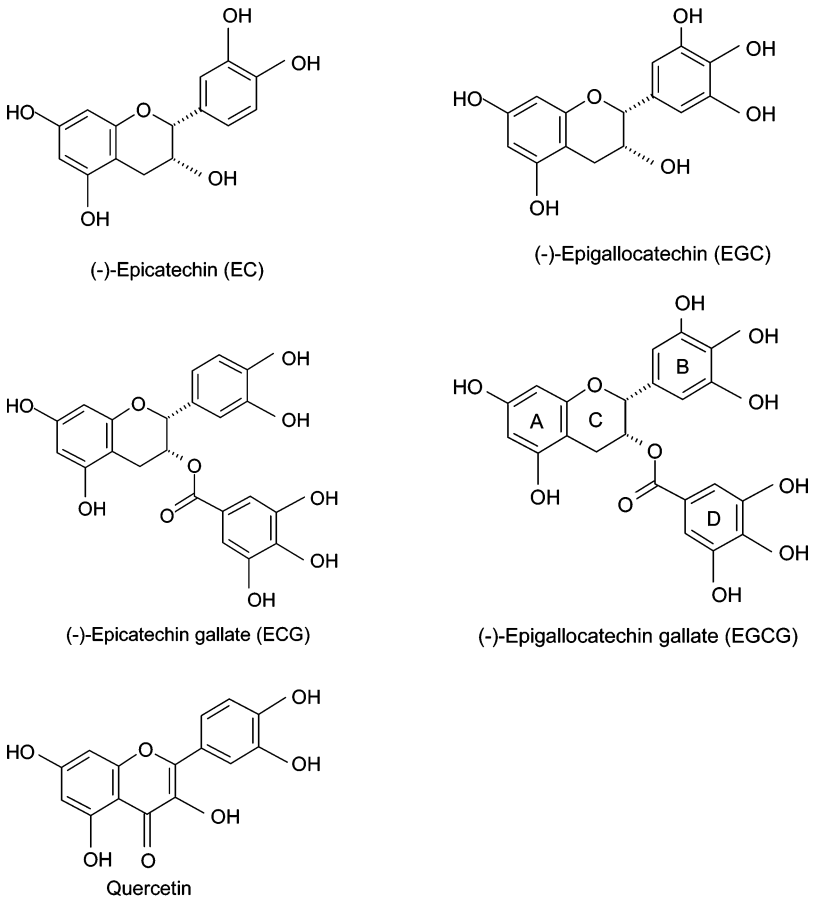

Figure 1. Chemical structures of the green tea catechins used in this study and quercetin.

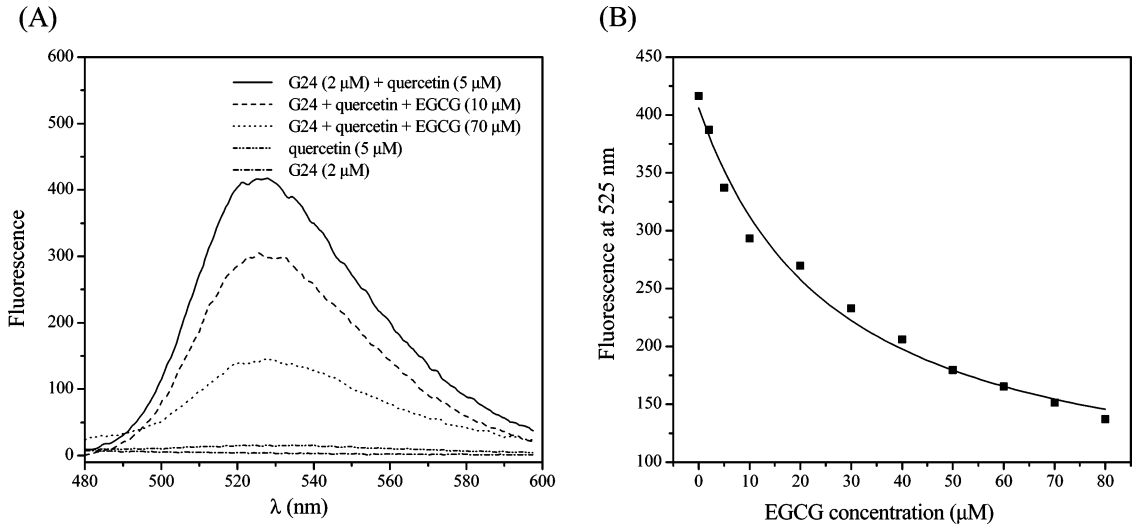

Figure 2. Displacement of fluorescent quercetin was used for monitoring the competitive binding of EGCG to the G24. (A) The fluorescent flavonoid quercetin binds to G24; its displacement with the nonfluorescent catechin EGCG caused fluorescence decreasing. (B) Determination of the dissociation constant (K_d) of EGCG. The decrease of fluorescence intensity at 525 nm was determined as a function of EGCG concentration. The line describes a nonlinear fitted curve of experimental data. The correction of the obtained K_{app} value using the equation from the Experimental Section gave a $K_{d(EGCG)}$ of 23 ± 3 μM.

and quenched in the aqueous buffer solution. Addition of catechins to quercetin as a control did not affect its fluorescence. The highest affinity for binding to G24 was determined for EGCG. The fluorescence titration of the G24−quercetin complex with EGCG is shown in Figure 2B. The fit of data and correction of K_{app} revealed a K_d of 23 ± 3 μM, close to the value of quercetin. The affinities of EGC, ECG, and EC to G24 were lower (respective K_d values of 34 ± 4, 36 ± 3, and 54 ± 5 μM).

Inhibition of ATPase Activity of Gyrase B. Occupation of the ATP-binding site by a catechin molecule is expected to result in inhibition of the ATPase activity. The ATPase activity of gyrase B in the presence of catechins was determined by monitoring NADH consumption in the coupled assay with pyruvate kinase and lactate dehydrogenase. Inhibition of the ATPase activity of gyrase B decreased in the following order: EGCG > ECG > EGC, while the presence of EC in reaction mixture did not decrease the ATPase activity (Figure 3). K_M

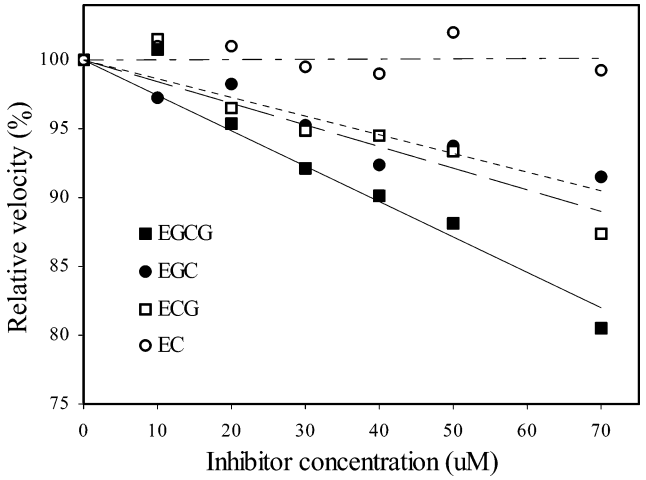

Figure 3. Inhibition of gyrase B ATPase activity is dependent on catechin concentration. The ATP hydrolysis was inhibited by catechins EGCG, ECG, EGC, but not by EC. The velocity of ATP hydrolysis in absence of catechins was defined as 100%.

for ATP is in the millimolar range; therefore, the presence of 3 mM ATP in the ATPase assay decreased the apparent inhibition of catechins due to the competition for the same binding site.

Inhibition of the DNA Supercoiling Activity of Gyrase. ATP hydrolysis is the driving force of DNA supercoiling by gyrase. Relaxed DNA was used as a substrate for gyrase, and formation of supercoiled DNA in the presence of catechins was detected by agarose electrophoresis. Figure 4 shows that green tea extract efficiently inhibited DNA supercoiling activity, giving the credence to the use of tea in the mouth hygiene. EGCG and ECG inhibited the formation of supercoiled DNA with estimated IC_{50} of 50 μM. Novobiocin was used as a positive control. EGC and EC did not inhibit gyrase up to concentrations of 100 μM (data not shown). To exclude the mode of inhibition through binding of catechins to DNA, we have assayed the ability of catechins to displace DNA-binding dyes Picogreen (Molecular probes, Eugene, OR) or ethidium bromide. None of the tested substances were able to displace the dyes from DNA (data not shown).

Structural Analysis of the G24−EGCG Complex Using NMR. To obtain structural data on contacts between G24 and EGCG we performed NMR [^{15}N,^{1}H]-HSQC titration experiments using [^{15}N]-labeled G24 in the presence of increasing amounts of unlabeled EGCG. With this approach, amide groups in G24 that display a chemical shift change upon addition of EGCG yield information about the protein−ligand interactions in the complex formed. The ratios of G24/EGCG ranged from 2:1 to 1:4 in an attempt to push the association equilibrium toward the bound state of the complex. The unlabeled EGCG component produced changes in chemical shift values and/or intensities of defined G24 amide peaks for backbone as well as side-chain amides of G24. The latter, however, were not included in the data analysis because of the relatively small magnitude of the chemical shift changes and reduced reproducibility of the results. With the exception of a cluster of residues around the binding site, the vast majority of amide cross-peaks showed no change, indicating that G24 remained structurally unaltered. For the amide groups of G24 that show no overlap in the HSQC spectra, the chemical shift changes in the ^{1}H and ^{15}N dimensions were combined according to the expression mentioned in the Experimental Section. The amide signals that were most strongly influenced (i.e., either shifted and/or reduced in intensity) belonged to Ile48, Gly75, Arg76, Gly77, Gly119, Gly164, and Met166 (displayed in Figure 5). In Figure 6, the

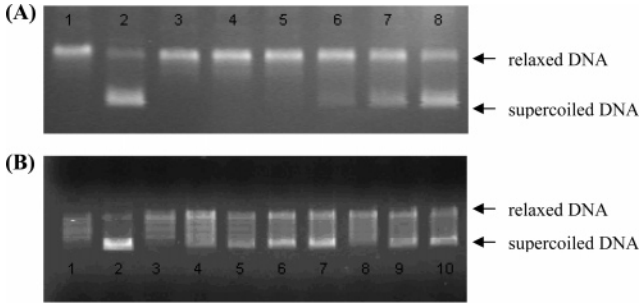

Figure 4. Inhibition of gyrase supercoiling activity by catechins. Control reactions were performed by incubation of relaxed DNA without (lines 1) and with (lines 2) gyrase as well as in the presence of 10^{-6} M novobiocin (lines 3). (A) The inhibition of gyrase was achieved by catechins from green tea extract. Extract was diluted before incubation and the concentration of green tea was as follows: 1.7, 0.67, 0.34, 0.17, and 0.048 μg of tea/μL reaction mixture (lines 4−8). (B) Inhibition of gyrase activity was determined in the presence of catechins EGCG and ECG. The catechins were included in the reaction mixture with relaxed gyrase as follows: EGCG at concentrations of 1×10^{-4} M, 5×10^{-5} M, 2×10^{-5} M, 1×10^{-5} M (lines 4−7) and ECG at concentrations of 1×10^{-4} M, 5×10^{-5} M and 1×10^{-5} M (lines 8−10).

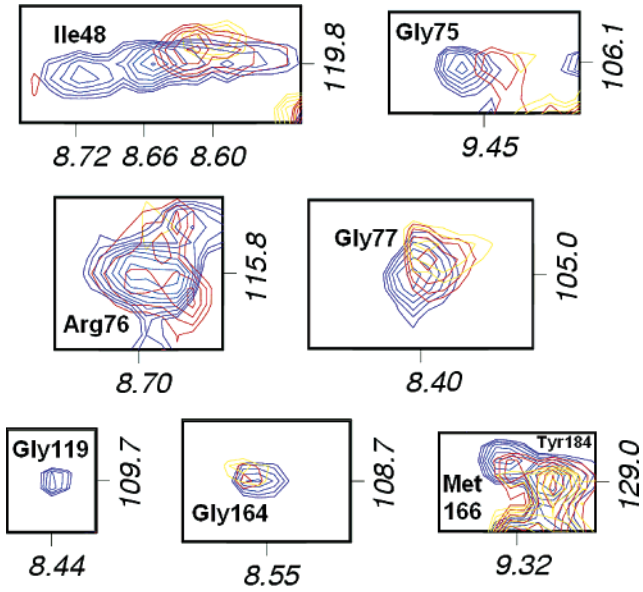

Figure 5. Parts of overlaid [^{15}N,^{1}H]-HSQC spectra of G24 recorded in the absence (blue) and presence of unlabeled EGCG (red, 1:1 and yellow, 1:4 molar ratio). The residues of G24 are labeled. In the bottom right panel, the unperturbed signal of Tyr184 is also shown.

corresponding residues are visualized on the backbone ribbon of G24.

Molecular Modeling. The AutoDock[40] calculations were performed with the grid centered at the biocin (the saccharide portion of novobiocin) binding site. A total of 100 structures of the G24−EGCG complex were calculated. The 10 best structures according to the AutoDock free-energy scoring function converged to two separate clusters of bound conformations of EGCG that both occupied the biocin binding site; a representative of each cluster bound to G24 and overlaid with novobiocin from ref 4 for comparison, are shown in Figure 6A,B, respectively.

Calculation of the target function counting the number of G24 residues with strong chemical shift perturbation in contact with EGCG showed that the structure from Figure 6A scored a significantly higher target function than the structure in Figure 6B because of residues 48 and 119 of G24, which have no

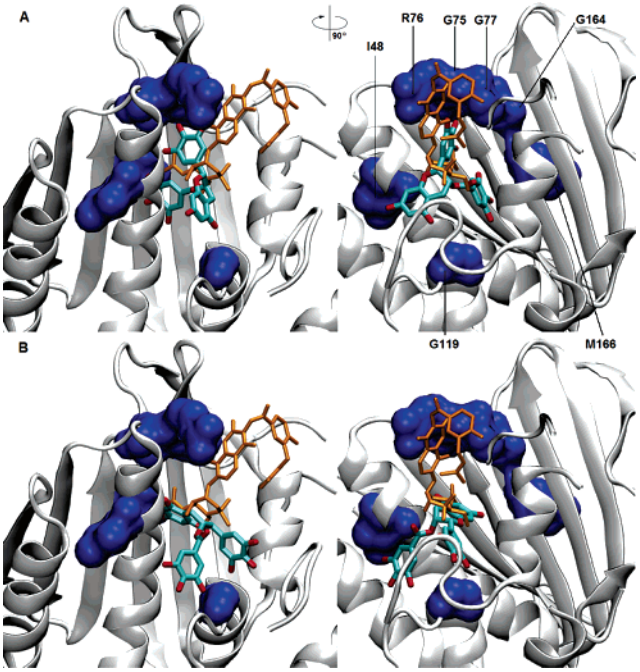

Figure 6. The G24 structure (PDB ID 1AJ6, as cartoon, including the well-known inhibitor novobiocin, as sticks, in orange) displaying the residues from Figure 5 that show strongest chemical shift perturbation upon addition of EGCG (spacefilled, in blue; for clarity, only the affected backbone amides are highlighted) and the representatives of two separate clusters of bound conformations of EGCG with best AutoDock final docking energies (A and B, respectively, as sticks in cyan and red). The display on the right is rotated by 90° about the vertical axis (clockwise, seen from above).

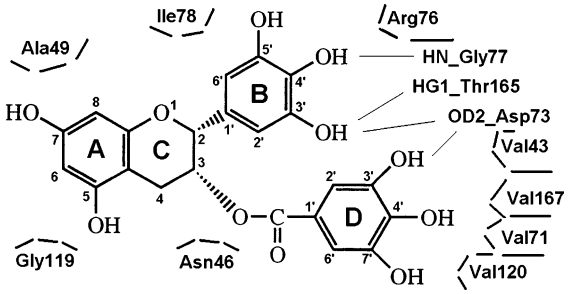

Figure 7. Two-dimensional display of G24 residues that interact with EGCG in the binding mode as shown in Figure 6A. Hydrogen bonds are shown explicitly.

contact with EGCG in the second cluster of structures. According to the combined results from docking and NMR, the most probable structure of the G24−EGCG complex is displayed in Figure 6A; more details of the interaction with G24 are schematically shown in Figure 7. The benzopyran function (rings A and C) enters the biocin binding site, while rings D and B reach toward Ile48 and Gly77, respectively, using their hydroxyl functions to form favorable contacts with protein atoms. Ring A, due to its planar structure, enters more deeply into the G24 interior than the biocin portion of novobiocin, also forming favorable contacts with its hydroxyl functions.

Discussion

Green tea catechins that have numerous pharmacological activities are among the most studied plant polyphenols. There is an extensive amount of data on the biological and biochemical activities of green tea extracts, including reports on the interaction with more than 20 protein targets, most of them enzymes, but also membrane proteins and cytoskeletal components. Much of the research has been focused on the activity of EGCG as the main polyphenolic constituent of green tea. This is in contrast to the paucity of the structural characterization of complexes of EGCG with its partners by experimental methods, with no structure of EGCG in complex with any protein being available. The closest approximation is the crystal structure of lipoxygenase in complex with a degradation product of EGCG;[41] additionally, a solution study of EGCG with a proline-rich peptide[42] and a molecular modeling study of the EGCG complex with proteasome,[43] DHFR,[44] and urokinase[45] have been reported.

Based on the binding of catechins to protein kinases[46] and hsp90,[47] we tested the hypothesis that EGCG could inhibit bacterial gyrase. Gyrases are essential bacterial proteins and their inactivation results in bacterial death. In the case of gyrase-catalyzed reactions DNA has been proposed as the main binding target of flavonoids. Our previous experiments showed that the flavonoid quercetin also binds to the ATP binding site of gyrase B, inhibiting DNA supercoiling activity.[37,48] In contrast to the planar quercetin that also binds to DNA,[49] EGCG does not produce DNA cleavage as do quinolones and quercetin. We have determined the binding of individual catechins to the G24 indirectly, utilizing fluorescent properties of quercetin to analyze this interaction. Displacement of quercetin with catechins in the complex with G24 caused the decrease of its fluorescence. The affinity of G24 was highest for EGCG and somewhat weaker for the other three catechins. In addition to the direct binding study, the inhibition of ATPase activity as well as inhibition of DNA supercoiling activity confirmed the biological effect of catechins on bacterial gyrase. The best inhibitive activity was displayed by EGCG, followed by ECG and EGC, while EC showed no inhibition in either ATPase or supercoiling assay. This result correlated with a measurement of antimicrobial activity, where the MIC for *E. coli* were 10, 25, 100, and >1000 μM for EGCG, ECG, EGC, and EC, respectively (data not shown). Among the catechins EGCG, most closely followed by ECG, showed the highest activity in all reported binding or inhibition assays, in accord with previously reported values.[28] The position as well as number of hydroxyl groups on catechins is important for gyrase inhibition, as shown by the different activities of EGC and EC that differ in a single hydroxyl group. Similar differences were already observed before for flavonoids.[50]

Berger et al. reported previously that EGCG inhibits topoisomerase I but not topoisomerase II in several human colon carcinoma cell lines.[51] Several studies comparing the *in vitro* cytotoxicity revealed that EGCG as well as ECG show toxicity to many cancers without affecting normal cells.[52−54] Catechins have antimicrobial activity at relatively high concentrations, particularly against Gram-negative bacteria due to the poor penetration of the bacterial outer membrane, which is evident in the highest antimicrobial activity against *E. coli* strains that possess more permeable outer membranes (DC2, UB1005; data not shown).

Concentrations of catechins in tea are well in their effective antimicrobial ranges,[29] and gyrase was inhibited already at 0.17 mg/mL of tea extract (Figure 4), which substantiates its application in oral hygiene. It is likely that bacterial gyrase is not the only target but probably one of the several targets in bacteria, with their relative importance differing between the bacterial strains.

To understand the molecular interaction between EGCG and DNA gyrase, and possibly other protein targets, we performed a solution NMR study of this interaction. With 220 residues present in G24, a significant overlap of amide signals in the

[^{15}N,^{1}H]-HSQC spectra is observed. Fortunately, many chemical shift perturbations occurred in the region of the spectrum with a small degree of overlap, for example, the region where most of the Gly residues are found ($\delta 15_N$ < 110 ppm). Those perturbations were not random shifts, but signify chemical shielding effects due to the presence of EGCG, as shown by the consistent direction of change with increasing EGCG concentration for selected peaks (Figure 5). The residues that show the strongest perturbations are located close to the novobiocin binding site (Figure 6). The cleft that can accommodate the novobiocin molecule can also accommodate the galloyl (ring D) or benzopyran ring (rings A−C) of EGCG (Figure 6B,A, respectively). In the only published structure of an EGC−protein complex[41] the EGC molecule is completely surrounded by lipoxygenase residues and also forms numerous intermolecular contacts with its hydroxyl functions. In our ATPase and binding assay, EGC was able to interact with gyrase, which is probably due to the large number of interactions originating from the B ring. In another docking study of EGCG and chymotrypsin, similarly to the present study, the fairly hydrophobic A−C rings of EGCG were proposed to be positioned in the S1 pocket of the 5-subunit, the galloyl group (ring D) above Ser 131 forming several intermolecular contacts, while the B ring projected up into solvent, bridging the two walls of the binding cleft.[43] The crucial role of the galloyl group in intramolecular contacts was proposed also in another recent modeling study with the catalytic site of the human DNA methyltransferase.[55]

In our study the residues Gly164 and Met166 of G24 are situated at the opposite side of the protein relative to the ATP/novobiocin binding site and are not in direct contact with EGCG; the intermolecular interaction with EGCG that leads to perturbation of the magnetic environments of their amide groups is probably relayed via Thr165 that is in close contact with O3 of ring B and O7 of ring A (Figure 7). The signal of the Thr165 amide in the HSQC spectra overlaps with those of Ser127 and Lys129, and its chemical shift perturbation cannot be confirmed; however, even in its absence the relay mechanism would remain probable because intermolecular contacts do not necessarily lead to detectable chemical shift change. Similar relay mechanisms that led to chemical shift perturbations on the side opposite to the contact surface were described in recent studies of protein−protein complexes.[56,57] A distinct binding site close to residues Gly164 and Met166 is much less probable according to the absence of any other chemical shift perturbations in their vicinity; nonspecific binding would most probably not be able to cause such large effects.

In the absence of intermolecular NMR data, the two structures of the G24−EGCG complex (Figure 6A,B) have equal probability according to AutoDock, however, the NMR data strongly favors the first and, in combination with computational data, uniquely identifies the mode of EGCG binding (Figures 6A and 7). A recent study using similar methods showed that an indolinone derivative binds to the ATP binding site of G24.[58] Structural and docking studies may be extended to other targets displaying structural similarity with gyrase B, such as hsp90.[59] EGCG as a lead may be able to avoid the toxicity of other antimicrobial agents directed against gyrase B to eukaryotic cells, such as coumarine derivatives. Additionally, the structural data presented in this report may provide the base for modification of this versatile scaffold to increase its specificity.

Overlay of EGCG with novobiocin (Figure 6) reveals that both molecules occupy the same binding site of gyrase B, directly suggesting potentially beneficial modifications of certain functional groups either of the catechins or novobiocin; the latter could benefit from a trihydroxyphenyl group at the 3′ position of the noviose ring of novobiocin, while in the former ring D of EGCG could be replaced by a pyrrole group, which is found at 3′ position of clorobiocin. The interaction of the galloyl group (ring B) with the conserved Arg76 residue of gyrase B could be strengthened by the introduction of an acidic group; this site of gyrase B, however, is often mutated in the novobiocin resistant bacterial strains. Contrary to the coumarines or the previously published quercetin,[37] the catechin scaffold is not planar, allowing the tri/dihydrohyphenyl groups of rings B and D to enter separate binding sites at almost perpendicular angles. Extension of ring B into the site occupied by the isopentenyl group of novobiocin that occupies part of the proposed hydrophobic binding site[60] could additionally increase the affinity and specificity. An extension of the A ring that overlaps with the ribose of ADPNP could interact with residues that bind to the hydroxyl groups of the ribose. An attractive perspective for improvement of the affinity would be the use a combinatorial library based on the catechin scaffold with variations of substituents at rings B and D; for the latter substituents, low affinity compounds identified by fragment-based discovery such as SAR by NMR or needles[61] could be particularly suitable.

Experimental Section

Materials. Production of recombinant gyrase A and B and the G24 was carried out in *Escherichia coli* strain BL21(DE3). Quercetin (Sigma) was dissolved in ethanol to the concentration of 5 mM and used as a fluorescent probe. Green tea catechins (Figure 1), EC, EGC, ECG, and EGCG, were purchased from Sigma. Stock solutions were prepared by dissolving compounds in ethanol at concentrations of 5 mM. Green tea extract was prepared as follows: 1 g of tea was extracted in 100 mL of water at 80 °C for 15 min. In the gyrase supercoiling activity assay, the extract was diluted for 6, 15, 30, 60, and 120 times.

Production and Isolation of Recombinant Gyrase A, B, G24, and ^{15}N Isotope Labeling of G24. The preparation of recombinant gyrase A, B, and G24 was described previously.[37] Some modifications were made, and the procedure was performed as follows: production of recombinant proteins was carried out in *E. coli* strain BL21(DE3) that was grown in LB medium at 37 °C and 180 rpm. For ^{15}N-labeled G24, the strain was grown in the M9 minimal medium containing $(^{15}NH_4)SO_4$. The protein production was induced by the addition of 0.4 mM IPTG at the OD of 0.5, and the fermentation was allowed to proceed for three additional hours. Cells were suspended in the lysis buffer containing 1 mM EDTA, 0.5 mM PMSF, and 0.1% Na-deoxycholate in 10 mM Tris buffer, pH 8.0. Cell suspension was placed on ice and sonication was performed for 5 min using TMX400 cell disruptor (Tekmar). Insoluble material was removed by centrifugation at 20.000 rpm and 4 °C for 30 min. Active recombinant gyrase A and B as well as G24 were purified from supernatant by the same protocol. DNA was precipitated by the addition of streptomycin to 4% and removed by centrifugation. Supernatant with 2 mM DTT was applied to the novobiocin−Sepharose column. The column was washed with buffer containing 20 mM Tris and 500 mM NaCl at pH 8.0 until the absorbance of the eluate at 280 nm decreased below 0.02. Proteins were eluted by 8 M urea in 20 mM Tris at pH 7.5. Fractions were diluted to absorbance of 0.1 with elution buffer and EDTA; DTT was added to the concentration of 1 mM. Refolding was performed by dialysis against buffer containing 20 mM K_3PO_4 at pH 7.2, 100 mM NaCl, 1 mM EDTA, 5% glycerol, and 0.02% NaN_3 at 4 °C, with several buffer exchanges. Proteins were concentrated in an Amicon cell with a 3 kDa cut off membrane. Gyrase A, B, G24, and ^{15}N-labeled G24 were stored at −80 °C in buffer in aliquots at concentrations of 1 mg/mL, 1 mg/mL, and 5 mg/mL, respectively. The correct fold of the proteins was confirmed by ATPase activity as well as by dispersion of NMR cross-peaks in HSQC spectra.

Fluorescence Measurements. Fluorescence measurements were performed with a LS55 spectrofluorimeter (Perkin-Elmer) with a double monochromator. All measurements were done at 25 °C in a 5 mm × 5 mm quartz cell equipped with a magnetic mixer. A slit width of 5 nm was used for both excitation and emission. Fluorescence titrations were carried out at an excitation wavelength of 370 nm, and emission spectra from 400 to 600 nm were recorded. Maximum emission was observed at 525 nm. To determine the dissociation constants of catechins, the quercetin-displacement method was used. Amounts equal to 2 μM G24 and 5 μM quercetin were incubated for 30 min at 25 °C and then titrated with catechin. An apparent dissociation constant (K_{app}) was obtained by performing a nonlinear fit of acquired data. With the use of the known dissociation constant for quercetin ($K_{d(querc)} = 15$ μM[37]), we calculated the K_d of catechins using the equation

$$K_{d(catechin)} = K_{app}/(1 + [querc]/K_{d(querc)})$$

Absorption spectra of catechins were measured to exclude the inner filter effect in fluorescence titration measurements.

ATPase Activity Assay. The ATPase activity of gyrase B was determined using a coupled assay of the enzymes pyruvate kinase and lactate dehydrogenase.[62] The hydrolysis of ATP was coupled with NADH oxidation and consumption of NADH was followed spectrophotometrically at 340 nm. The reaction mixture in a total volume of 1 mL was composed of 5 mM β-mercaptoethanol, 4 mM phosphoenolpyruvate, 0.32 mM NADH, 13 U of pyruvate kinase, 27 U of lactate dehydrogenase, 250 μg/mL bovine serum albumin, 150 mM potassium acetate, 8 mM $MgCl_2$, and 250 nM gyrase B in 50 mM Hepes buffer at pH 7.5. The catechins were added in a range of 0−70 μM, and the mixture was preincubated for 30 min at 37 °C. The reaction was started with the addition of 3 mM ATP; the absorbance at 340 nm was measured for 5 min.

Measurement of Inhibition of Gyrase Supercoiling Activity. The supercoiling assay measures the transformation of the relaxed form of plasmid DNA into a supercoiled conformation, based on the difference in the mobility in gel electrophoresis. The inhibition of gyrase supercoiling activity was determined in a reaction mixture containing the following: 35 mM Tris (pH 7.5), 24 mM KCl, 4 mM $MgCl_2$, 0.36 mg/mL bovine serum albumin, 9 μg/mL tRNA, 6.5% glycerol, 5 mM DTT, 1.4 mM ATP, 1.8 mM spermidine, 10 μg/mL relaxed pUC19 DNA, 1 U of mixture of gyrase A and B from *E. coli*, and different concentrations of catechins in the range of 1×10^{-4} M to 1×10^{-5} M. In the case of green tea extract, the prepared extract was added in dilution range from 6 to 480 times. The total volume of reaction was 20 μL. For control, performing the reaction without any catechin proved the activity of the gyrase, and novobiocin (10^{-6} M) was added instead of catechins. After 20 min of incubation at 37 °C, the reaction was terminated by the addition of 2 μL of proteinase K (10 mg/mL) and 2 μL of SDS (2%). The samples were analyzed by electrophoresis using 1.0% agarose gel and Tris-borate buffer (90 mM Tris-borate and 2 mM EDTA). After 1 h of electrophoresis at 100 V, the gel was stained with ethidium bromide and observed under UV light.

Determination of Antibacterial Activity of Compounds. Standard minimum inhibitory concentrations (MIC) were determined by the microdilution assay following the recommendations of the Clinical and Laboratory Standards Institute (CLSI, formerly NCCLS). Briefly, serial twofold dilutions of the compounds were made in LB medium and 100 μL/well of each dispensed into 96-well U-bottom microtiter plates (TPP, Trasadingen, Switzerland). Fresh bacteria (*E.coli*, strains DC2 and UB1005, 18−20 h cultures on LB agar) were suspended in saline at an $O.D._{600}$ of 0.04 (1×10^7 CFU/mL, approximately), a 100-fold dilution prepared in LB medium, and 100 μL/well dispensed. Incubation was carried out at 37 °C for 18−20 h without shaking, and the MIC was visually determined.

NMR Measurements. The NMR samples contained 0.44 mM ^{15}N-labeled G24, 20 mM potassium phosphate buffer (pH 7.2), 100 mM NaCl, 0.1% azide, and 5% D_2O. The G24 sample was titrated in consecutive steps using 7 μL of EGCG stock solution (1.42 mg/309.6 μL) leading to G24/EGCG molar ratios of 2:1, 1:1, 1:2, and finally 1:4. All NMR measurements were carried out on a Varian 600 Inova spectrometer equipped with a 5-mm triple-resonance gradient probe. 2D sensitivity-enhanced [^{15}N,^{1}H]-HSQC experiments were recorded at 30 °C with 1024 and 256 complex data points in the ^{1}H and ^{15}N dimensions, respectively. The spectral widths were set to 8000 (^{1}H) and 2000 Hz (^{15}N), respectively. Protons were referenced to internal DSS, and the ^{15}N dimension was calibrated indirectly with respect to the proton chemical shift.[63] After identification of the amide signals on the basis of previous resonance assignments[48] and peak fitting using FELIX (Accelrys, Inc., San Diego, U.S.A.), EGCG-induced changes in the backbone amide proton ($\Delta\delta^1$HN) and nitrogen ($\Delta\delta^{15}$N) chemical shifts of G24 were determined and combined according to Mulder et al.,[64] using the expression $\sqrt{[(\Delta\delta^1\text{HN})2 + (\Delta\delta^{15}\text{N})2/6.5]}$. These combined chemical shift changes were normalized to a maximum of 100%. The residues with the strongest chemical shift perturbations were selected using a threshold of 0.02 ppm for the chemical shift change (comparing the spectra without EGCG and with G24/EGCG ratio of 1:4). They were also selected in the case that the amide signal significantly (>50%) lost intensity upon addition EGCG.

Molecular Modeling. The coordinates of the novobiocin-resistant mutant (R136H) of the N-terminal 24 kDa fragment[4] (PDB ID 1AJ6) and the coordinates of EGCG prepared in INSIGHT II (Accelrys, Inc., San Diego, U.S.A) were used for molecular docking calculations with the program AutoDock.[40] The protein was kept rigid while in EGCG all 11 rotatable bonds were defined as flexible using the *deftors* module of AutoDock. AutoDock performs the docking of the ligand to a set of grid points describing the target protein; the AutoGrid calculation was run with 98 points (separated by 0.275 Å) in each spatial dimension, using atom C28 of novobiocin in 1AJ6 as center of the grid for the AutoDock calculation. The latter was run using the Lamarckian Genetic Algorithm with a translation step (*tstep*) of 0.2 Å, a quaternion step (*qstep*) of 5.0 deg, and a torsion step (*tstep*) of 5.0 deg, producing 100 structures that were evaluated in the analysis step. Here a target function was calculated for each docked structure that added a 1 for each residue of G24 perturbed in chemical shift that was in close contact (<2.2 Å) to any atom of EGCG. The docked structure with lowest final docked energy and the highest target function was selected as the most probable G24−EGCG complex.

Acknowledgment. NMR experiments were performed at the Slovenian NMR Center at the National Institute of Chemistry. The AutoDock calculations were performed at the Vrana supercomputer cluster at the National Institute of Chemistry, Ljubljana. This project was financed by a grant from the Slovenian Research Agency. We thank Robert Bremšak and Iva Bratkovič Hafner for their help in the preparation of gyrase.

References

(1) Lambert, P. A. Bacterial resistance to antibiotics: Modified target sites. *Adv. Drug Delivery Rev.* **2005**, *57*, 1471−1485.
(2) Kampranis, S. C.; Maxwell, A. The DNA gyrase−quinolone complex. ATP hydrolysis and the mechanism of DNA cleavage. *J. Biol. Chem.* **1998**, *273*, 22615−22626.
(3) Maxwell, A. DNA gyrase as a drug target. *Trends Microbiol.* **1997**, *5*, 102−109.
(4) Lewis, R. J.; Singh, O. M.; Smith, C. V.; Skarzynski, T.; Maxwell, A.; Wonacott, A. J.; Wigley, D. B. The nature of inhibition of DNA gyrase by the coumarins and the cyclothialidines revealed by X-ray crystallography. *EMBO J.* **1996**, *15*, 1412−1420.
(5) Hirano, R.; Sasamoto, W.; Matsumoto, A.; Itakura, H.; Igarashi, O.; Kondo, K. Antioxidant ability of various flavonoids against DPPH radicals and LDL oxidation. *J. Nutr. Sci. Vitaminol.* **2001**, *47*, 357−362.
(6) Kemberling, J. K.; Hampton, J. A.; Keck, R. W.; Gomez, M. A.; Selman, S. H. Inhibition of bladder tumor growth by the green tea derivative epigallocatechin-3-gallate. *J. Urol.* **2003**, *170*, 773−776.
(7) Kinjo, J.; Nagao, T.; Tanaka, T.; Nonaka, G.; Okawa, M.; Nohara, T.; Okabe, H. Activity-guided fractionation of green tea extract with antiproliferative activity against human stomach cancer cells. *Biol. Pharm. Bull.* **2002**, *25*, 1238−1240.

(8) Yamamoto, T.; Lewis, J.; Wataha, J.; Dickinson, D.; Singh, B.; Bollag, W. B.; Ueta, E.; Osaki, T.; Athar, M.; Schuster, G.; Hsu, S. Roles of catalase and hydrogen peroxide in green tea polyphenol-induced chemopreventive effects. *J. Pharmacol. Exp. Ther.* **2004**, *308*, 317−323.
(9) Calixto, J. B.; Campos, M. M.; Otuki, M. F.; Santos, A. R. Anti-inflammatory compounds of plant origin. Part II. Modulation of pro-inflammatory cytokines, chemokines and adhesion molecules. *Planta Med.* **2004**, *70*, 93−103.
(10) Chyu, K. Y.; Babbidge, S. M.; Zhao, X.; Dandillaya, R.; Rietveld, A. G.; Yano, J.; Dimayuga, P.; Cercek, B.; Shah, P. K. Differential effects of green tea-derived catechin on developing versus established atherosclerosis in apolipoprotein E-null mice. *Circulation* **2004**, *109*, 2448−2453.
(11) Miura, Y.; Chiba, T.; Tomita, I.; Koizumi, H.; Miura, S.; Umegaki, K.; Hara, Y.; Ikeda, M.; Tomita, T. Tea catechins prevent the development of atherosclerosis in apoprotein E-deficient mice. *J. Nutr.* **2001**, *131*, 27−32.
(12) Kazi, A.; Smith, D. M.; Zhong, Q.; Dou, Q. P. Inhibition of bcl-x(l) phosphorylation by tea polyphenols or epigallocatechin-3-gallate is associated with prostate cancer cell apoptosis. *Mol. Pharmacol.* **2002**, *62*, 765−771.
(13) Smith, D. M.; Wang, Z.; Kazi, A.; Li, L. H.; Chan, T. H.; Dou, Q. P. Synthetic analogs of green tea polyphenols as proteasome inhibitors. *Mol. Med.* **2002**, *8*, 382−392.
(14) Adhami, V. M.; Ahmad, N.; Mukhtar, H. Molecular targets for green tea in prostate cancer prevention. *J. Nutr.* **2003**, *133*, 2417S−2424S.
(15) Chen, D.; Daniel, K. G.; Kuhn, D. J.; Kazi, A.; Bhuiyan, M.; Li, L.; Wang, Z.; Wan, S. B.; Lam, W. H.; Chan, T. H.; Dou, Q. P. Green tea and tea polyphenols in cancer prevention. *Front. Biosci.* **2004**, *9*, 2618−2631.
(16) Conney, A. H.; Lu, Y.; Lou, Y.; Xie, J.; Huang, M. Inhibitory effect of green and black tea on tumor growth. *Proc. Soc. Exp. Biol. Med.* **1999**, *220*, 229−233.
(17) Fujiki, H. Two stages of cancer prevention with green tea. *J. Cancer Res. Clin. Oncol.* **1999**, *125*, 589−597.
(18) Cao, Y.; Cao, R.; Brakenhielm, E. Antiangiogenic mechanisms of diet-derived polyphenols. *J. Nutr. Biochem.* **2002**, *13*, 380−390.
(19) Fassina, G.; Vene, R.; Morini, M.; Minghelli, S.; Benelli, R.; Noonan, D. M.; Albini, A. Mechanisms of inhibition of tumor angiogenesis and vascular tumor growth by epigallocatechin-3-gallate. *Clin. Cancer Res.* **2004**, *10*, 4865−4873.
(20) Akiyama, H.; Fujii, K.; Yamasaki, O.; Oono, T.; Iwatsuki, K. Antibacterial action of several tannins against Staphylococcus aureus. *J. Antimicrob. Chemother.* **2001**, *48*, 487−491.
(21) Gibbons, S.; Moser, E.; Kaatz, G. W. Catechin gallates inhibit multidrug resistance (MDR) in Staphylococcus aureus. *Planta Med.* **2004**, *70*, 1240−1242.
(22) Kono, K.; Tatara, I.; Takeda, S.; Arakawa, K.; Hara, Y. Antibacterial activity of epigallocatechin gallate against methicillin-resistant Staphylococcus aureus. *Kansenshogaku Zasshi* **1994**, *68*, 1518−1522.
(23) Matsunaga, K.; Klein, T. W.; Friedman, H.; Yamamoto, Y. Legionella pneumophila replication in macrophages inhibited by selective immunomodulatory effects on cytokine formation by epigallocatechin gallate, a major form of tea catechins. *Infect. Immun.* **2001**, *69*, 3947−3953.
(24) Taguri, T.; Tanaka, T.; Kouno, I. Antimicrobial activity of 10 different plant polyphenols against bacteria causing food-borne disease. *Biol. Pharm. Bull.* **2004**, *27*, 1965−1969.
(25) Yanagawa, Y.; Yamamoto, Y.; Hara, Y.; Shimamura, T. A combination effect of epigallocatechin gallate, a major compound of green tea catechins, with antibiotics on Helicobacter pylori growth in vitro. *Curr. Microbiol.* **2003**, *47*, 244−249.
(26) Yoda, Y.; Hu, Z. Q.; Zhao, W. H.; Shimamura, T. Different susceptibilities of Staphylococcus and Gram-negative rods to epigallocatechin gallate. *J. Infect. Chemother.* **2004**, *10*, 55−58.
(27) Zhao, W. H.; Asano, N.; Hu, Z. Q.; Shimamura, T. Restoration of antibacterial activity of beta-lactams by epigallocatechin gallate against beta-lactamase-producing species depending on location of beta-lactamase. *J. Pharm. Pharmacol.* **2003**, *55*, 735−740.
(28) Amarowicz, R.; Pegg, R. B.; Bautista, D. A. Antibacterial activity of green tea polyphenols against *Escherichia coli* K 12. *Nahrung* **2000**, *44*, 60−62.
(29) Hamilton-Miller, J. M. Antimicrobial properties of tea (Camellia sinensis L.). *Antimicrob. Agents Chemother.* **1995**, *39*, 2375−2377.
(30) Caturla, N.; Vera-Samper, E.; Villalain, J.; Mateo, C. R.; Micol, V. The relationship between the antioxidant and the antibacterial properties of galloylated catechins and the structure of phospholipid model membranes. *Free Radical Biol. Med.* **2003**, *34*, 648−662.
(31) Ikigai, H.; Nakae, T.; Hara, Y.; Shimamura, T. Bactericidal catechins damage the lipid bilayer. *Biochim. Biophys. Acta* **1993**, *1147*, 132−136.
(32) Tsuchiya, H. Effects of green tea catechins on membrane fluidity. *Pharmacology* **1999**, *59*, 34−44.
(33) Zhang, Y. M.; Rock, C. O. Evaluation of epigallocatechin gallate and related plant polyphenols as inhibitors of the FabG and FabI reductases of bacterial type II fatty-acid synthase. *J. Biol. Chem.* **2004**, *279*, 30994−31001.
(34) Ahn, H. Y.; Hadizadeh, K. R.; Seul, C.; Yun, Y. P.; Vetter, H.; Sachinidis, A. Epigallocathechin-3 gallate selectively inhibits the PDGF-BB-induced intracellular signaling transduction pathway in vascular smooth muscle cells and inhibits transformation of *sis*-transfected NIH 3T3 fibroblasts and human glioblastoma cells (A172). *Mol. Biol. Cell* **1999**, *10*, 1093−1104.
(35) Sah, J. F.; Balasubramanian, S.; Eckert, R. L.; Rorke, E. A. Epigallocatechin-3-gallate inhibits epidermal growth factor receptor signaling pathway. Evidence for direct inhibition of ERK1/2 and AKT kinases. *J. Biol. Chem.* **2004**, *279*, 12755−12762.
(36) Gilbert, E. J.; Maxwell, A. The 24 kDa N-terminal sub-domain of the DNA gyrase B protein binds coumarin drugs. *Mol. Microbiol.* **1994**, *12*, 365−373.
(37) Plaper, A.; Golob, M.; Hafner, I.; Oblak, M.; Solmajer, T.; Jerala, R. Characterization of quercetin binding site on DNA gyrase. *Biochem. Biophys. Res. Commun.* **2003**, *306*, 530−536.
(38) Marcu, M. G.; Chadli, A.; Bouhouche, I.; Catelli, M.; Neckers, L. M. The heat shock protein 90 antagonist novobiocin interacts with a previously unrecognized ATP-binding domain in the carboxyl terminus of the chaperone. *J. Biol. Chem.* **2000**, *275*, 37181−37186.
(39) Meyer, P.; Prodromou, C.; Hu, B.; Vaughan, C.; Roe, S. M.; Panaretou, B.; Piper, P. W.; Pearl, L. H. Structural and functional analysis of the middle segment of hsp90: implications for ATP hydrolysis and client protein and cochaperone interactions. *Mol. Cell* **2003**, *11*, 647−658.
(40) Morris, G. M.; Goodsell, D. S.; Halliday, R. S.; Huey, R.; Hart, W. E.; Belew, R. K.; Olson, A. J. Automated Docking Using a Lamarckian Genetic Algorithm and Empirical Binding Free Energy Function. *J. Comput. Chem.* **1998**, *19*, 1639−1662.
(41) Skrzypczak-Jankun, E.; Zhou, K.; Jankun, J. Inhibition of lipoxygenase by (−)-epigallocatechin gallate: X-ray analysis at 2.1 A reveals degradation of EGCG and shows soybean LOX-3 complex with EGC instead. *Int. J. Mol. Med.* **2003**, *12*, 415−420.
(42) Charlton, A. J.; Haslam, E.; Williamson, M. P. Multiple conformations of the proline-rich protein/epigallocatechin gallate complex determined by time-averaged nuclear Overhauser effects. *J. Am. Chem. Soc.* **2002**, *124*, 9899−9905.
(43) Smith, D. M.; Daniel, K. G.; Wang, Z.; Guida, W. C.; Chan, T. H.; Dou, Q. P. Docking studies and model development of tea polyphenol proteasome inhibitors: Applications to rational drug design. *Proteins* **2004**, *54*, 58−70.
(44) Navarro-Peran, E.; Cabezas-Herrera, J.; Hiner, A. N.; Sadunishvili, T.; Garcia-Canovas, F.; Rodriguez-Lopez, J. N. Kinetics of the inhibition of bovine liver dihydrofolate reductase by tea catechins: origin of slow-binding inhibition and pH studies. *Biochemistry* **2005**, *44*, 7512−7525.
(45) Jankun, J.; Keck, R. W.; Skrzypczak-Jankun, E.; Swiercz, R. Inhibitors of urokinase reduce size of prostate cancer xenografts in severe combined immunodeficient mice. *Cancer Res.* **1997**, *57*, 559−563.
(46) Opare Kennedy, D.; Kojima, A.; Hasuma, T.; Yano, Y.; Otani, S.; Matsui-Yuasa, I. Growth inhibitory effect of green tea extract and (−)-epigallocatechin in Ehrlich ascites tumor cells involves a cellular thiol-dependent activation of mitogenic-activated protein kinases. *Chem. Biol. Interact.* **2001**, *134*, 113−133.
(47) Palermo, C. M.; Westlake, C. A.; Gasiewicz, T. A. Epigallocatechin gallate inhibits aryl hydrocarbon receptor gene transcription through an indirect mechanism involving binding to a 90 kDa heat shock protein. *Biochemistry* **2005**, *44*, 5041−5052.
(48) Golič Grdadolnik, S.; Oblak, M.; Šolmajer, T.; Jerala, R., Investigation of novel DNA gyrase inhibitors using the high resolution NMR spectroscopy. In *Drug discovery and design: medical aspects*; Matsoukas, J., Mavromoustakos, T., Eds.; IOS Press: Amsterdam, 2002; Vol. 55, pp 312−322.
(49) Austin, C. A.; Patel, S.; Ono, K.; Nakane, H.; Fisher, L. M. Site-specific DNA cleavage by mammalian DNA topoisomerase II induced by novel flavone and catechin derivatives. *Biochem. J.* **1992**, *282* (Pt 3), 883−889.
(50) Gutzeit, H. O.; Henker, Y.; Kind, B.; Franz, A. Specific interactions of quercetin and other flavonoids with target proteins are revealed by elicited fluorescence. *Biochem. Biophys. Res. Commun.* **2004**, *318*, 490−495.
(51) Berger, S. J.; Gupta, S.; Belfi, C. A.; Gosky, D. M.; Mukhtar, H. Green tea constituent (−)-epigallocatechin-3-gallate inhibits topoisomerase I activity in human colon carcinoma cells. *Biochem. Biophys. Res. Commun.* **2001**, *288*, 101−105.

(52) Ahmad, N.; Gupta, S.; Mukhtar, H. Green tea polyphenol epigallocatechin-3-gallate differentially modulates nuclear factor kappaB in cancer cells versus normal cells. *Arch. Biochem. Biophys.* **2000**, *376*, 338−346.
(53) Yang, G. Y.; Liao, J.; Kim, K.; Yurkow, E. J.; Yang, C. S. Inhibition of growth and induction of apoptosis in human cancer cell lines by tea polyphenols. *Carcinogenesis* **1998**, *19*, 611−616.
(54) Mittal, A.; Pate, M. S.; Wylie, R. C.; Tollefsbol, T. O.; Katiyar, S. K. EGCG down-regulates telomerase in human breast carcinoma MCF-7 cells, leading to suppression of cell viability and induction of apoptosis. *Int. J. Oncol.* **2004**, *24*, 703−710.
(55) Lee, W. J.; Shim, J. Y.; Zhu, B. T. Mechanisms for the Inhibition of DNA Methyltransferases by Tea Catechins and Bioflavonoids. *Mol. Pharmacol.* **2005**, *21*, 21.
(56) Wienk, H.; Maneg, O.; Lücke, C.; Pristovšek, P.; Löhr, F.; Ludwig, B.; Rüterjans, H. Interaction of cytochrome c with cytochrome c oxidase: An NMR study on two soluble fragments derived from Paracoccus denitrificans. *Biochemistry* **2003**, *42*, 6005−6012.
(57) Muresanu, L.; Pristovšek, P.; Löhr, F.; Maneg, O.; Mukrasch, M. D.; Rüterjans, H.; Ludwig, B.; Lücke, C. The electron transfer complex between cytochrome c552 and the CuA domain of the Thermus thermophilus ba3 oxidase. A combined NMR and computational approach. *J. Biol. Chem.* **2006**, *281*, 14503−14513.
(58) Oblak, M.; Grdadolnik, S. G.; Kotnik, M.; Poterszman, A.; Atkinson, R. A.; Nierengarten, H.; Desplancq, D.; Moras, D.; Solmajer, T. Biophysical characterization of an indolinone inhibitor in the ATP-binding site of DNA gyrase. *Biochem. Biophys. Res. Commun.* **2006**, *349*, 1206−1213.
(59) Prodromou, C.; Roe, S. M.; O'Brien, R.; Ladbury, J. E.; Piper, P. W.; Pearl, L. H. Identification and structural characterization of the ATP/ADP-binding site in the Hsp90 molecular chaperone. *Cell* **1997**, *90*, 65−75.
(60) Schechner, M.; Sirockin, F.; Stote, R. H.; Dejaegere, A. P. Functionality maps of the ATP binding site of DNA gyrase B: Generation of a consensus model of ligand binding. *J. Med. Chem.* **2004**, *47*, 4373−4390.
(61) Boehm, H. J.; Boehringer, M.; Bur, D.; Gmuender, H.; Huber, W.; Klaus, W.; Kostrewa, D.; Kuehne, H.; Luebbers, T.; Meunier-Keller, N.; Mueller, F. Novel inhibitors of DNA gyrase: 3D structure based biased needle screening, hit validation by biophysical methods, and 3D guided optimization. A promising alternative to random screening. *J. Med. Chem.* **2000**, *43*, 2664−2674.
(62) Tamura, J. K.; Gellert, M. Characterization of the ATP binding site on Escherichia coli DNA gyrase. Affinity labeling of Lys-103 and Lys-110 of the B subunit by pyridoxal 5′-diphospho-5′-adenosine. *J. Biol. Chem.* **1990**, *265*, 21342−21349.
(63) Wishart, D. S.; Bigam, C. G.; Yao, J.; Abildgaard, F.; Dyson, H. J.; Oldfield, E.; Markley, J. L.; Sykes, B. D. 1H, 13C and 15N chemical shift referencing in biomolecular NMR. *J. Biomol. NMR* **1995**, *6*, 135−140.
(64) Mulder, F. A.; Schipper, D.; Bott, R.; Boelens, R. Altered flexibility in the substrate-binding site of related native and engineered high-alkaline Bacillus subtilisins. *J. Mol. Biol.* **1999**, *292*, 111−123.

JM060817O